



Theoretical and spectroscopic investigations on the structure and bonding in B–C–N thin films

Erman Bengu^{a,*}, Mustafa F. Genisel^a, Oguz Gulseren^b, Rasim Ovali^b

^a *Bilkent University, Department of Chemistry, Ankara, Turkey*

^b *Bilkent University, Department of Physics, Ankara, Turkey*

ARTICLE INFO

Available online 9 October 2009

Keywords:

BCN
FTIR
XPS
TEM

ABSTRACT

In this study, we have synthesized boron, carbon, and nitrogen containing films using RF sputter deposition. We investigated the effects of deposition parameters on the chemical environment of boron, carbon, and nitrogen atoms inside the films. Techniques used for this purpose were grazing incidence reflectance-Fourier-transform infrared spectroscopy (GIR-FTIR), X-ray photoelectron spectroscopy (XPS), transmission electron microscopy (TEM) and electron energy loss spectroscopy (EELS). GIR-FTIR experiments on the B–C–N films deposited indicated presence of multiple features in the 600 to 1700 cm^{-1} range for the infrared (IR) spectra. Analysis of the IR spectra, XPS and the corresponding EELS data from the films has been done in a collective manner. The results from this study suggested even under nitrogen rich synthesis conditions carbon atoms in the B–C–N films prefer to be surrounded by other carbon atoms rather than boron and/or nitrogen. Furthermore, we have observed a similar behavior in the chemistry of B–C–N films deposited with increasing substrate bias conditions. In order to better understand these results, we have compared and evaluated the relative stability of various nearest-neighbor and structural configurations of carbon atoms in a single BN sheet using DFT calculations. These calculations also indicated that structures and configurations that increase the relative amount of C–C bonding with respect to B–C and/or C–N were energetically favorable than otherwise. As a conclusion, carbon tends to phase-segregate in to carbon clusters rather than displaying a homogeneous distribution for the films deposited in this study under the deposition conditions studied.

© 2009 Elsevier B.V. All rights reserved.

1. Introduction

B–C–N ternary system has been the focus of various studies concerned with the synthesis of materials with notable properties such as extreme hardness and low coefficient of friction. Some of the hardest materials known such as diamond, cubic-BN (c-BN), boron carbide (B_4C) and lubricious materials such as hexagonal-BN (h-BN) and graphite can be cited as examples to compounds in this system. Nevertheless, these are all compounds in the B–C–N ternary system with two components. (In the rest of the document “BCN” will be used to denote materials in the B–C–N ternary phase diagram with all three components.) One of the earliest reports on BCN materials was published by Gingerich [1] studying the heat atomization of a BCN molecule by mass spectrometry, whereas an early computational study on BCN compounds can be dated back to 1971 by Moffat [2]. In the same year, Kosolapova et al. [3] reported on the bulk solid synthesis of BCN compounds, which is followed by a proceedings report of Badzian et al. [4] for the CVD deposition of BCN films. Studies on the BCN compounds gained further interest after a computational study on the electronic properties of a BCN compound by Liu et al. [5].

Since then, various techniques ranging from high temperature/high pressure processing (HP/HT) [6], explosive compaction [7], pulsed-laser deposition [8], ion-beam assisted deposition [9] and magnetron sputtering [10] have been used for the synthesis of BCN materials in bulk or thin film format.

There have been reports in the literature regarding successful synthesis of atomically hybridized BCN films through analysis of spectroscopic data from mainly Fourier-transformed infrared spectroscopy (FTIR) and X-ray photoelectron spectroscopy (XPS) [11,12], while in others similar data sets have been interpreted as an indication for a phase segregation and presence of a phase mixture instead [10,13]. In this paper, we present a new approach for investigation of the bonding chemistry of BCN films. Although, we have also relied primarily on XPS and FTIR to understand the bonding chemistry of the films deposited, we have also used DFT calculations on simple atomic models of BCN films in order to gain further insight in the bonding chemistry and the structure.

2. Experimental

BCN films were deposited on single crystal Si (100) substrates through reactive RF magnetron sputtering using a B_4C target (Kurt Lesker, %99.9 purity) in an Ar/N_2 atmosphere. Before deposition Si

* Corresponding author. Tel.: +90 312 290 2153; fax: +90 312 266 4068.
E-mail address: bengu@fen.bilkent.edu.tr (E. Bengu).

(100) substrates were cleaned ex-situ using a special procedure for inducing a hydrogen terminated surface on the silicon substrates. Also to ensure cleanliness, all substrates were plasma cleaned for 15 min in the deposition chamber with an RF generated Ar plasma. First, a Ti buffer layer of approximately 200 nm thickness was sputter deposited on the substrates for improving the adhesion of BCN films to the substrate surface. Depositions of the BCN layer was carried at a pressure of 0.67 Pa and N_2 gas content in the system was kept at 10%. During deposition, with the help of a separate RF power supply unit a constant negative DC bias with respect to ground has been applied on the substrate. Grazing incidence reflection-FTIR (GIR-FTIR) technique [14] on a Bruker Hyperion 3000 FTIR microscope was employed for investigating the bonding characteristics of the BCN films due to the thick Ti buffer layer deposited under the BCN film. Additionally, all of the films were investigated using a Thermo Fisher Scientific K-Alpha XPS system with monochromated Al K_{α} . Prior to XPS investigation, surfaces of the BCN films were not ion-beam cleaned in the XPS equipment to avoid ion-beam induced mixing which may complicate interpretation of XPS data. Later on, cross-sectional transmission electron microscopy (TEM) samples were prepared from a number of the films to be used for TEM analysis in a JEOL JEM-2100FX equipped with a GATAN GIF Tridiem.

3. Results

In an FTIR spectrum, peak positions are determined by the strength of the bond between the two atoms and these atoms' relative masses. In addition, nearest neighbors of the atoms involved also define the chemical environment influencing the exact position of the respective peaks. In Fig. 1, FTIR spectra for the films deposited in this study are shown. A wide band between 900 and 1700 cm^{-1} were found to be the main feature for the films deposited for both grounded and floating substrates, other than the common features such as the B–N–B bending at 780 cm^{-1} . This wide band in the IR spectra for the BCN films deposited using floating and grounded substrate bias conditions encompasses the B–C, C–N and B–N stretching bands. However, as the negative DC bias applied to the substrate is increased, the intensity of this wide band region significantly diminishes and B–N stretching at around 1400 cm^{-1} becomes more obvious. Furthermore, another band at around 1500 to 1580 cm^{-1} , denoted in Fig. 1, gains strength for the films deposited using higher substrate bias values. Although, there have

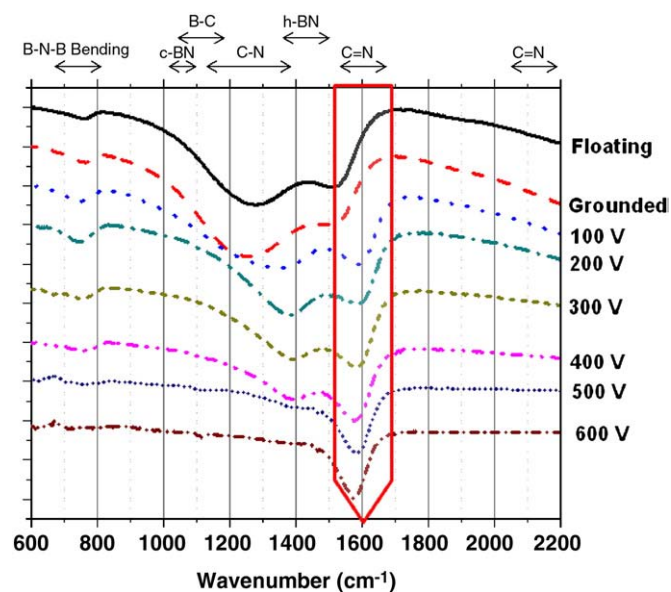


Fig. 1. GIR-FTIR spectra recorded from BCN films deposited using varying substrate bias settings. An unidentified band between 1500 and 1580 cm^{-1} exists for the BCN films deposited using substrate bias settings above -100 VDC .

been discussions on the identity of this peak [15], a consensus has not been reached definitively stating whether it is due to C–N or C–C bonding.

Examination of the XPS spectra around the B 1s, N 1s and C 1s regions of the deposited films provide more detail regarding the chemistry of the films. B 1s spectra of the films, as shown in the Fig. 2(a), does not indicate a significant change with substrate bias. For grounded and floating substrates a weak B–O component at 192.5 eV and a weaker B–C component at 189 eV are observed, as show in Fig. 2(b). N 1s spectra, on the other hand, suggest considerable local bonding chemistry changes occurring around the N atoms in the structure. As shown in Fig. 3(a), an atypical transition in the N 1s spectra can be observed going from BCN films deposited on floating and grounded substrates to BCN films synthesized on -100 VDC and higher biased substrates. N 1s spectrum for the BCN film synthesized on the grounded substrate can be explained by the convolution of two separate peaks; one positioned at a binding energy around 398.5 eV and the other positioned at 400.5 eV . Previous studies on BCN films identify the peak positioned at 398.5 eV for B–N bonding [11,12], and considered peak at 400.5 eV position in N 1s spectrum as an evidence for binding between N and sp^2 hybridized C atoms [11,12]. Hence, this finding indicates a local change in the bonding chemistry around N atoms in the BCN films. At lower substrate bias settings, higher intensity for the peak assigned for C–N together with the large band observed for FTIR spectra may suggest a relatively better hybridized environment where all three components are bonded to each other. At higher substrate bias, C–N peak seems to shift toward 400 eV , possibly due to less C atoms around the N atoms. C 1s spectra from the BCN films (stacked) as shown in Fig. 4(a) and (b) do not indicate a noteworthy change in components and shape upon variation in substrate bias.

In addition to changes in the bonding chemistry, evidence for changes in the atomic structure and chemical composition of the BCN films deposited at various substrate bias settings were examined. TEM image and EELS spectrum from the BCN film deposited using grounded substrate suggest an amorphous structure as shown in Fig. 5(a), which is in contrast to the films deposited using higher substrate bias settings, such as the BCN film for -200 VDC bias shown in Fig. 5(b). For the films deposited at bias settings other than grounded and floating substrates, the structure of the BCN films bear a significant resemblance to turbostratic-BN (t-BN) layers observed for c-BN films where the c-axis of the growing individual h-BN sheets are parallel to the substrate surface [16]. Furthermore, B to C atomic ratio in the BCN films, calculated from the quantification of EELS spectra gathered during TEM analysis, Fig. 6, decreases by the increase in substrate bias, hence carbon amount in the film deposited at -400 VDC bias approximately doubled with respect to that of BCN film deposited at on a grounded substrate.

In order to understand the film structures, we have performed the first principles plane-wave calculations [17] within density functional theory (DFT) [18,19] by the projector-augmented-wave (PAW) potentials [20,21] using Vienna ab-initio simulation package (VASP) program [22–24]. The exchange-correlation potential was expressed in terms of the generalized gradient approximation (GGA) (Perdew-Wang 91 type [25]). To achieve the desired accuracy, a plane-wave cutoff energy of 500 eV was used in all calculations. A BN large supercell with 10 \AA of vacuum is introduced to minimize the ion-ion interaction in the non-periodic directions. Therefore, only the Γ point is used as Monkhorst–Pack [26] mesh in order to model the k-point sampling in the Brillouin zone. The partial occupancy around the Fermi level is treated by Gaussian smearing with a smearing parameter of 0.08 eV . For all calculations energy was converged to within 10^{-4} eV accuracy. In all calculations, edges of finite sized structures are saturated by H atoms and then all of the atoms are relaxed to their minimum energy configurations by using conjugate gradient method where total energy and atomic forces are minimized. Maximum force magnitude remained on each atom is set at most to 0.06 eV/\AA .

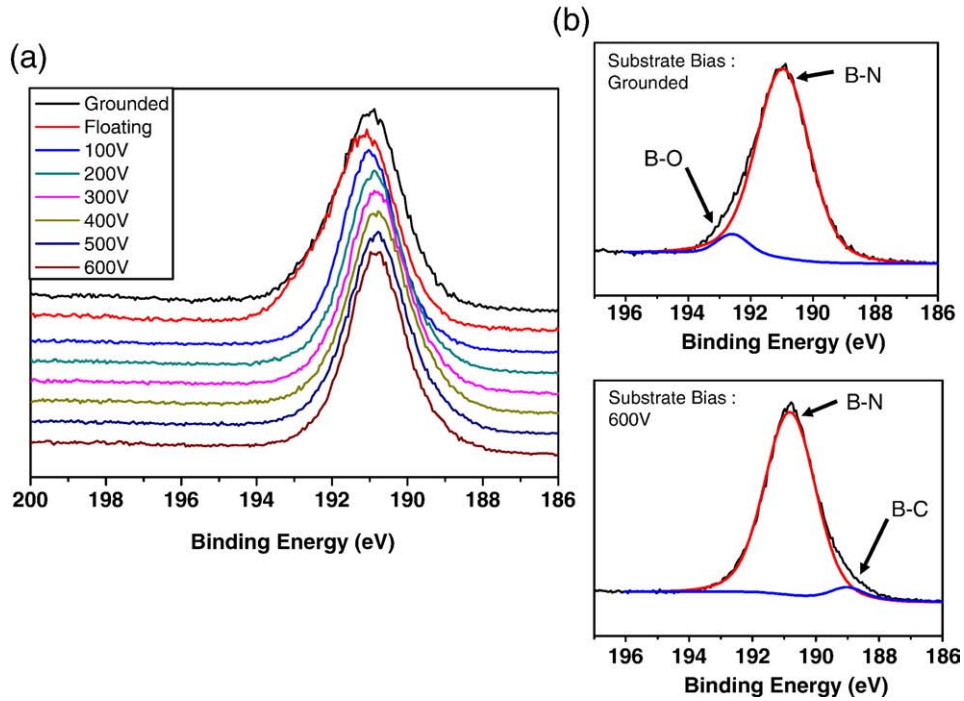


Fig. 2. (a) B 1s XPS spectra from BCN films deposited at increasing substrate bias settings. (b) B 1s spectra from two representative films (grounded and –600 V bias setting) have been each fit with two Gaussians components.

In order to quantify the various C substituted BN films, the energy of defects per atom is calculated through first principles. Here, we define the defect energy as follows:

$$E_{def}[BN - C] = E_{tot}[BN - C] - E_{tot}[BN] - n_C\mu_C + n_B\mu_B + n_N\mu_N \quad (1)$$

where E_{tot} is the total energy of the corresponding system, n 's are the difference number of atoms with respect to the perfect BN films for

each species and μ_C, μ_B and μ_N are the chemical potentials for carbon, boron and nitrogen respectively. Metallic alpha-boron phase for B and gas phases for N and H were used to calculate the corresponding chemical potentials. We show the calculated defect energies of various carbon substituted in the model BN supercell in Table 1. The resulting defect energy values indicate the stability of a carbon ring structure and aggregation of carbon atoms by taking advantage of C–C bond. For example, as in the cases of 6 and 7 carbon atoms substituted, defect

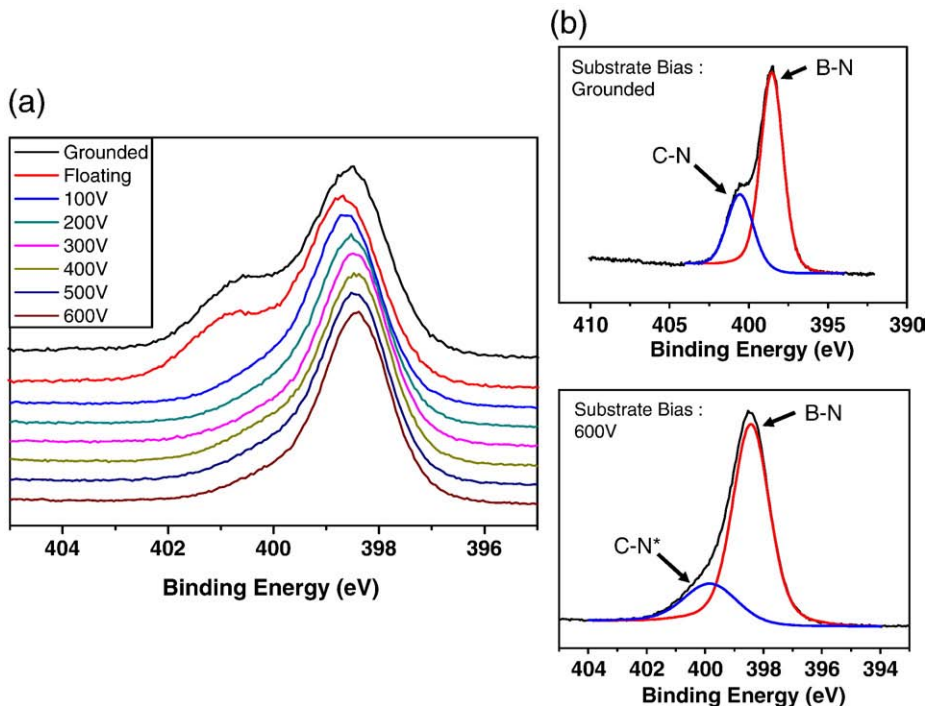


Fig. 3. (a) N 1s XPS spectra from BCN films deposited at increasing substrate bias settings. (b) N 1s spectra from two representative films (grounded and –600 V bias setting) have been each fit with two Gaussians components. There is a 0.5 eV shift measured for the C–N peak (denoted with C–N*) for the BCN film deposited at –600 VDC substrate bias.

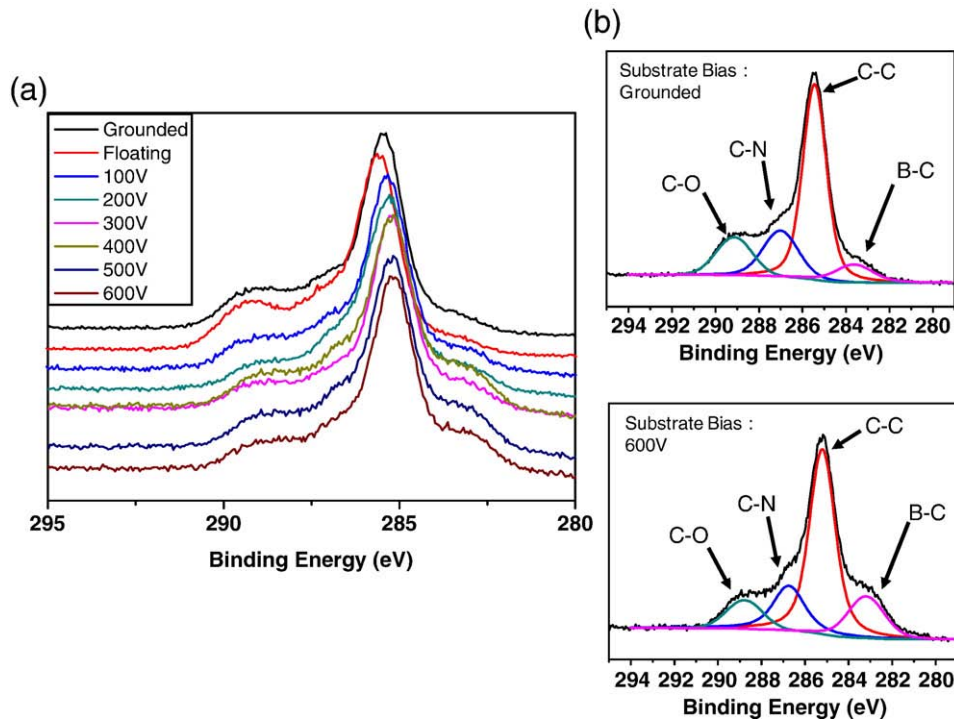


Fig. 4. (a) C 1s XPS spectra from BCN films deposited at increasing substrate bias settings. (b) C 1s spectra from two representative films (grounded and –600 V bias setting) have been each fit with four Gaussians components.

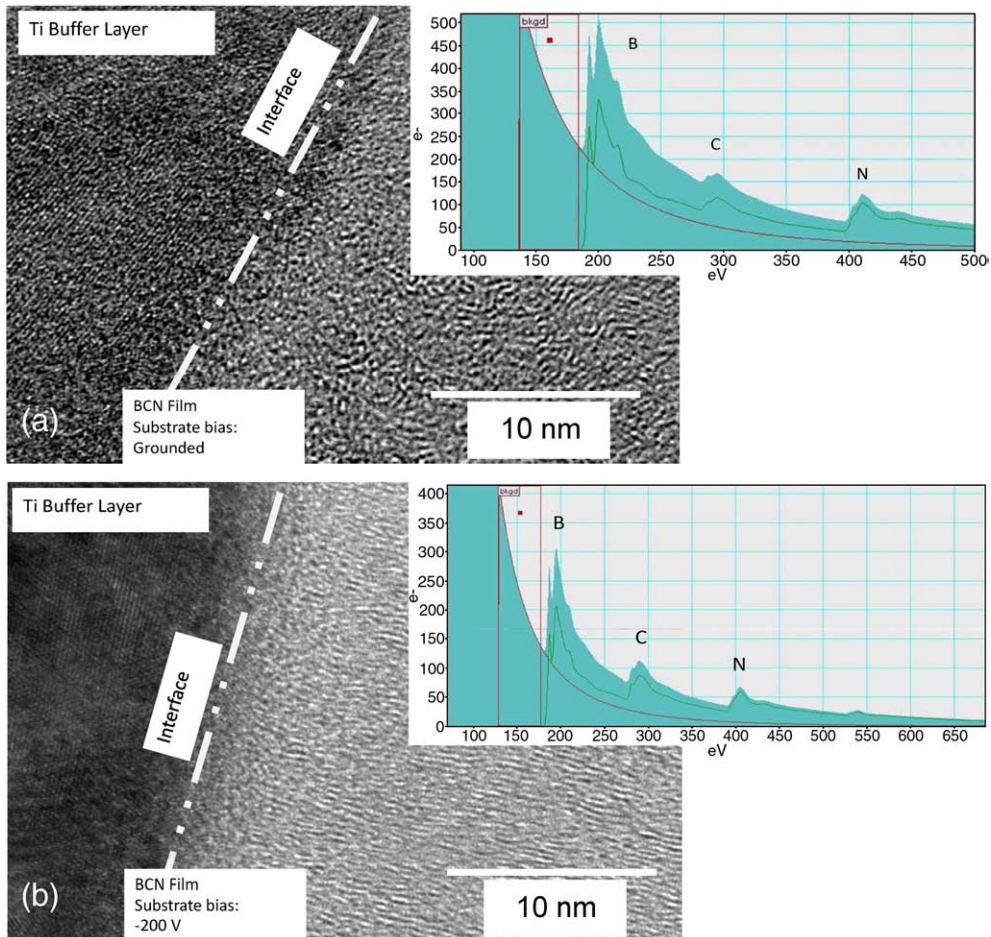


Fig. 5. (a) TEM image of the BCN film deposited using a grounded substrate suggests an amorphous atomic structure. (b) BCN films deposited at a substrate bias of –200 VDC indicates a t-BN like atomic structure. Insets show EELS spectra from both films.

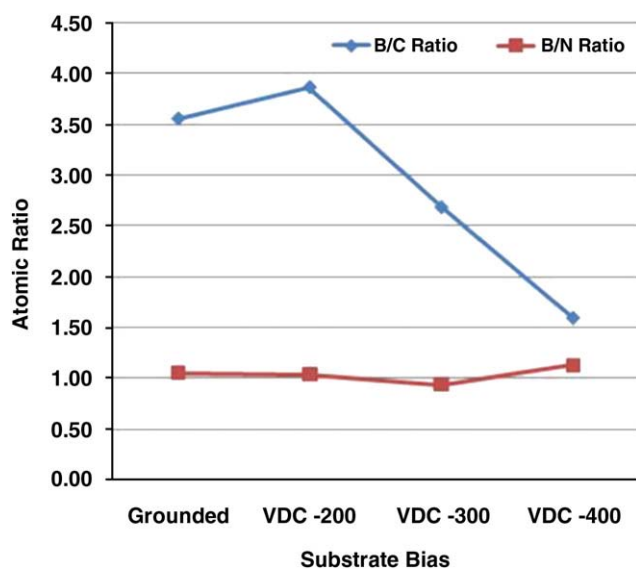


Fig. 6. The effect of substrate bias on the B/C atomic ratio and B/N atomic ratio.

energy is roughly 1 eV lower when a complete ring of carbon atoms is formed instead of the carbon chain structures. On the other hand, when the number of carbon atoms is not enough to form a complete ring in the case of 5 carbon atom substitutions as shown in Fig. 7, defect energies are similar for the chain and incomplete ring-like defect structures. Furthermore, a careful evaluation of the defect energies for the chain and ring-like cases in 5 carbon atom structures show that even in this case there is an energy penalty of 0.36 eV when the carbon atoms form an incomplete ring. In the case of 7 carbon atom defects, if the 7th carbon atom is isolated from the carbon ring, the total of the defect increases indicating that C–C bonds are energetically favored by the system.

4. Conclusion

In conclusion, results of our studies indicate that when lower substrate bias is used during deposition, BCN films assume an amorphous structure with a chemical bonding state close to hybridization where all atomic species are bonded to each other. However, at higher substrate bias values the film structure reverts to a mixture of two distinct phases; a carbon rich phase and the h-BN phase. This is very likely to be due to the excess energy imparted by the impinging ions on the growing film increasing as the bias is increased on the substrate. Hence, under these conditions atoms in the growing film can have higher activation energy to find energetically more suitable positions and neighbors. Therefore, at the higher substrate bias settings, the resultant film structure is dominated by energetically more favorable C–C and B–N bonds which lead to sp² bonded layered soft hexagonal networks. These findings are supported by DFT calculations showing carbon rings energetically being more stable than the same number of individual carbon atoms in a hexagonal network.

Table 1
Various carbon substituted BN films and their defect energies.

| Structure | Defect energy (eV) |
|--------------|--------------------|
| 5C chain | 11.16 |
| 5C ring-like | 11.52 |
| 6C chain | 12.25 |
| 6C ring | 10.86 |
| 7C chain | 14.82 |
| 7C ring | 13.78 |

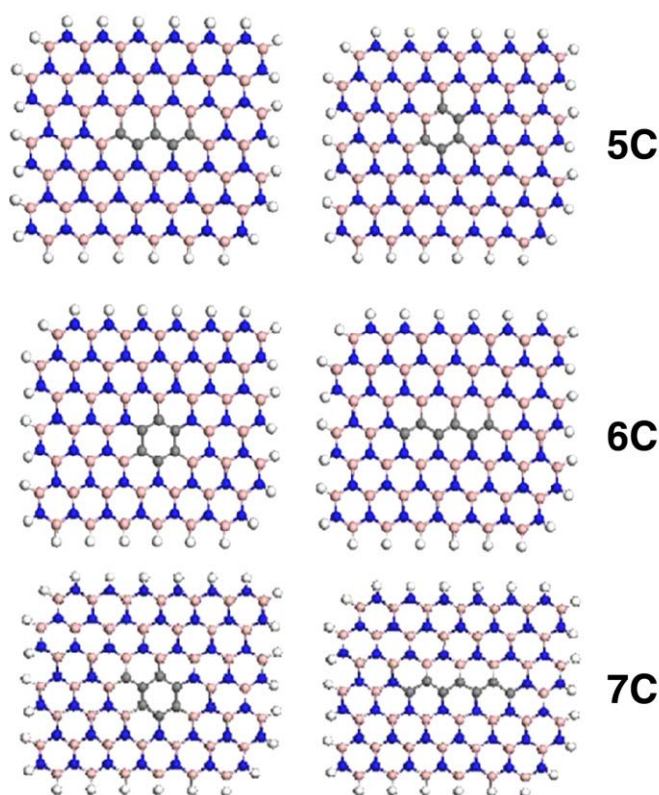


Fig. 7. Three different carbon concentrations are shown, 5 carbon atoms at the first row, 6 carbon atoms at the second row and 7 carbon atoms at the bottom row. Atom labels are as follows: hydrogen (white), boron (pink), nitrogen (blue), and carbon (black). (For interpretation of the references to color in this figure legend, the reader is referred to the web version of this article.)

Acknowledgements

The authors would like to acknowledge financial support for the work by TUBITAK (Grant no: 106T328 and 107T892) and European Union 7. Framework project Unam-Regpot (Grant no: 203953).

References

- [1] K.A. Gingerich, *J. Chem. Soc. D: Chem. Comm.* 1 (1969) 764.
- [2] J.B. Moffat, *J. Mol. Structure* 7 (1971) 474.
- [3] T. Ya, G.N. Makarenko, Kosolapova, T.I. Serebryakova, E.V. Prilutskii, O.T. Khorpyakov, O.I. Chernysheva, *Poroshkovaya Metallurgiya* 1 (1971) 27.
- [4] A.R. Badzian, T. Niemyski, S. Appenheimer, E. Olkuskni, in *Proceedings of the International Conference on Chemical Vapor Deposition*, edited by F.A. Glaski, Vol.3 (American Nuclear Society, Hinsdale, IL, 1972), p.747.
- [5] A.Y. Liu, R.M. Wentzcovitch, M.L. Cohen, *Phys. Rev. B* 39 (1989) 1760.
- [6] S. Nakano, M. Akaishi, T. Sasaki, S. Yamaoka, *Chemistry of Materials* 6 (1994) 2246.
- [7] Y. Zhao, D.W. He, L.L. Daemen, T.D. Shen, R.B. Schwarz, Y. Zhu, D.L. Bish, J. Huang, J. Zhang, G. Shen, J. Qian, T.W. Zerda, *Journal of Materials Research* 17 (2002) 3139.
- [8] H. Ling, J.D. Wu, J. Sun, W. Shi, Z.F. Ying, F.M. Li, *Diamond and Related Materials* 11 (2002) 1623.
- [9] R. Gago, I. Jimenez, J.M. Albella, L.J. Terminello, *Applied Physics Letters* 78 (2001) 3430.
- [10] V. Linss, S.E. Rodil, P. Reinke, M.G. Garnier, P. Oelhafen, U. Kreissig, F. Richter, *Thin Solid Films* 467 (2004) 76.
- [11] L. Liu, Y. Wang, K. Feng, Y. Li, W. Li, C. Zhao, Y. Zhao, *Applied Surface Science* 252 (2006) 4185.
- [12] P.-C. Tsai, *Surface and Coatings Technology* 201 (2007) 5108.
- [13] S. Ulrich, H. Ehrhardt, T. Theel, J. Schwan, S. Westermeyr, M. Scheib, P. Becker, H. Oechsner, G. Dollinger, A. Bergmaier, *Diamond and Related Materials* 7 (1998) 839.
- [14] R.G. Greenler, *J. Chem. Phys.* 44 (1966) 310.
- [15] V. Linss, I. Hermann, N. Schwarzer, U. Kreissig, F. Richter, *Surface and Coatings Technology* 163–164 (2003) 220.
- [16] D.J. Kester, R. Messier, *J. Appl. Phys.* 72 (1992) 504.
- [17] M.C. Payne, M.P. Teter, D.C. Allen, T.A. Arias, J.D. Joannopoulos, *Review of Modern Physics* 64 (1992) 1045–1097.
- [18] W. Kohn, L.J. Sham, *Phys. Rev.* 140 (1965) A1133.

- [19] P. Hohenberg, W. Kohn, *Phys. Rev.* 136 (1964) B864.
- [20] P.E. Blöchl, *Phys. Rev. B* 50 (1994) 17953.
- [21] G. Kresse, D. Joubert, *Phys. Rev. B* 59 (1999) 1758.
- [22] Computations have been carried out with the VASP software: G. Kresse and J. Hafner, *Phys. Rev. B*, 48 (1993) 13115–13118.
- [23] G. Kresse, J. Furthmüller, *Comput. Mater. Sci.* 6 (1996) 15.
- [24] G. Kresse, J. Furthmüller, *Phys. Rev. B* 54 (1996) 11169.
- [25] J.P. Perdew, J.A. Chevary, S.H. Vosko, K.A. Jackson, M.R. Pederson, D.J. Singh, C. Fiolhais, *Phys. Rev. B* 46 (1992) 6671.
- [26] H.J. Monkhorst, J.D. Pack, *Phys. Rev. B* 13 (1976) 5188.